

Chapter 3

Conformal Mapping Technique

Various techniques have been used to calculate the conductor loss, including Wheeler's incremental inductance rule [26], closed-form formulae based on rigorous numerical techniques and interpolation [27], perturbation methods combined with the conformal mapping technique [28-35], quasi-static and full-wave approaches based on the spectral domain method (SDM) [36], integral equation method (IEM) [37], finite element method (FEM) [38], mode-matching method (MMM) [39, 40], etc. When the conductor thickness is the order of the skin depth, traditional quasi-analytic Wheeler's incremental inductance rule and classical conformal mapping models become inadequate to characterize the attenuation, since they assume the conductor thickness is much larger than the skin depth. Rigorous quasi-static and full-wave numerical techniques give accurate frequency dependent parameters, such as characteristic impedance and complex propagation constant from DC to high frequency, but these are numerically intensive and time-consuming.

Recently, an efficient quasi-static technique has been developed to calculate the conductor loss by using the conformal mapping technique [21, 22], which is based on quasi-TEM approximation. This technique was applied to a coplanar waveguide (CPW) and symmetric twin conductors, and calculated resistance agreed well to experimental data for all frequencies. This technique is accurate for mirror symmetric structures, even though good results were obtained for the asymmetric structure of a coplanar waveguide (CPW). In the previous work the conductor thickness was assumed zero in the conformal mapping procedure and the surface impedance of a flat

conductor (i.e., position independent) was used for the effective internal impedance all over the conductor surfaces in case of a coplanar waveguide (CPW). In this chapter, this technique will be applied to examples of a microstrip line and a V-shaped conductor backed coplanar waveguide (VGCPW), while considering the conductor thickness in the conformal maps and using the EII of thick rectangular conductors. The calculated resistance and inductance are compared to the results of more rigorous quasi-static solutions. And it is explained that the effective internal impedance (EII) approximates the standard impedance boundary condition (SIBC) and this technique gives a reasonable approximation in the asymmetric problems of a microstrip and a V-shaped conductor backed coplanar waveguide (VGCPW).

3.1 Conformal Mapping and Partial Differential Equations

A point in the w -plane can be related to a given point in the z -plane with a function. Any point (x, y) in the z -plane yields some point (u, v) in the w -plane, and the function that accomplishes this is called a coordinate transformation from the z -plane to w -plane. If the function consists of complex variables and is analytic, then a complex plane of $z = x + jy$ is transformed into another complex plane of $w = u + jv$, and the infinitesimal shape is preserved during the transformation. This is called a conformal map, and the Cauchy-Riemann conditions of (3.1) is a sufficient and necessary condition for that function to be a conformal map.

$$\begin{aligned}\frac{\partial u}{\partial x} &= \frac{\partial v}{\partial y} \\ \frac{\partial u}{\partial y} &= -\frac{\partial v}{\partial x}\end{aligned}\tag{3.1}$$

A conformal map can transform a complicated domain to a simple domain through a given function;

$$w = f(z) \quad (3.2)$$

And a potential function ϕ that is a solution to the Laplace equation defined in the z -plane can be converted to a potential function ψ defined in the w -plane. By invoking the Cauchy-Riemann conditions to replace variable z in ϕ by w , the invariance of Laplace equation under a conformal transformation is shown in the reference [41] by

$$\frac{\partial^2 \phi(x, y)}{\partial x^2} + \frac{\partial^2 \phi(x, y)}{\partial y^2} = \frac{1}{M^2} \left(\frac{\partial^2 \psi(u, v)}{\partial u^2} + \frac{\partial^2 \psi(u, v)}{\partial v^2} \right) = 0 \quad (3.3)$$

$$M = \left| \frac{dw}{dz} \right|$$

where M is a scaling factor that is the derivative of the mapping function with respect to z . These transformations can be done through any number of intermediate steps to get a simpler and more readily analyzable configuration, and many physical problems that depend on the Laplace equation can be easily solved. Therefore, finding a complex function mapping the original domain into the simple domain replaces solving a Laplace equation in original domains. Many transmission lines have been analyzed using conformal maps to give characteristic impedance and effective permittivity in case of lossless thin conductors.

For the lossy conductor of finite conductivity and finite thickness, the conformal map should transform the region inside of the conductor as well as outside of the conductor to consider the field penetration into the conductor. And a scalar Helmholtz equation is added as a governing partial differential equation inside the conductor as well as the Laplace equation outside of the conductor. The Helmholtz equation is modified under the transformations to become

$$\nabla_{xy}^2 J(x, y) - j\omega\mu\sigma J(x, y) = \frac{1}{M^2} \left(\nabla_{uv}^2 \tilde{J}(u, v) - j\omega\mu\sigma M^2 \tilde{J}(u, v) \right) = 0 \quad (3.4)$$

where a complicated inhomogeneous conductivity should be considered in the mapped domain. The simplification of the boundaries is accompanied by the complexity of inhomogeneous conductor material properties, and this trade-off makes it as hard to analyze lossy transmission lines in the mapped domains as it was in the original domains.

The perturbation method combined with the conformal mapping technique can be used to calculate the conductor loss [28-35], but these techniques are valid only at high frequency where the conductor thickness is larger than the skin depth. In the following section, a method using the conformal mapping technique is presented which can find the conductor loss from low frequency where the conductor thickness is on the order of the skin depth or less to high frequency where the skin and proximity effect are fully developed.

3.2 Conductor Loss Calculation using Conformal Mapping Technique

To accurately predict frequency dependent resistance and inductance the model should account for not only current crowding towards the surface and edges of the conductor due to the skin and proximity effect at high frequency, but also uniform current distribution at low frequency. To avoid conformal maps inside of the conductor and properly consider the frequency dependent skin depth, a complex EII is defined on the surface of the conductor, which represent resistance and internal inductance of conductors and is determined by the frequency and the geometry, permittiv-

ity, permeability, and conductivity of the isolated conductor. And to account for the current crowding induced by the interaction between and inside of the conductors (i.e., the proximity effect), a conformal map transforms the complicated real space domain into a simple domain and the transverse resonance method is then applied. This approach is valid up to the frequency where the quasi-TEM assumption is appropriate, and the calculation of capacitance and effective permittivity is decoupled from the calculation of resistance and inductance.

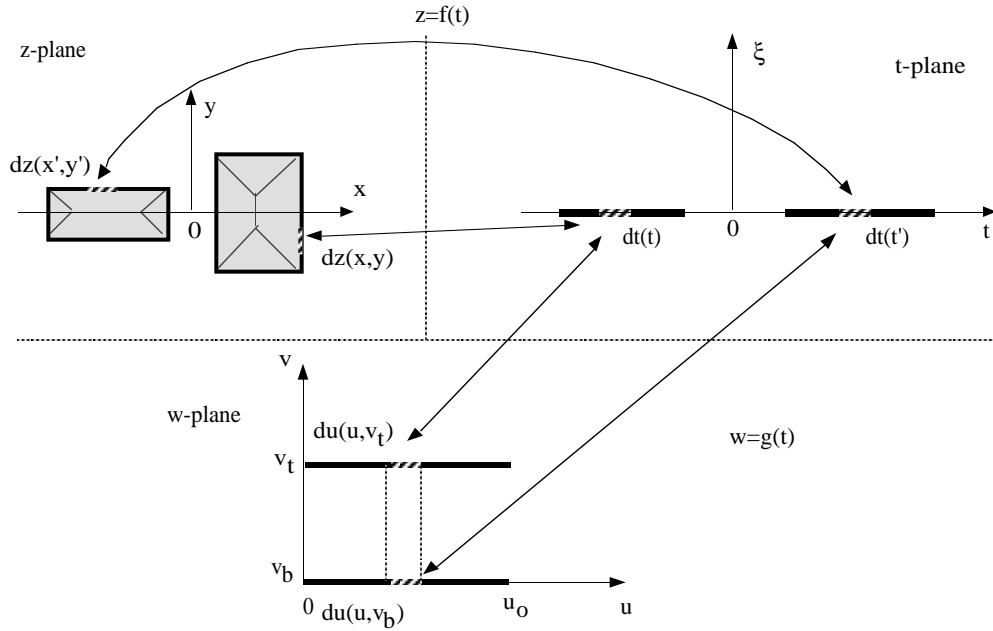


Figure 3.1: Conformal mapping process from the original plane (z -plane) to the intermediate plane (t -plane), and finally to the mapped plane (w -plane).

3.2.1 Conformal Mapping Technique using Effective Internal Impedance and Transverse Resonance Method

In Fig. 3.1 two rectangular conductors in the z -plane are mapped into infinitesimally thin coplanar strips in the intermediate t -plane with a map of $z = f(t)$ and fi-

nally mapped into parallel plates in the w -plane with a map of $w = g(t)$. A point (x, y) on the surface of the conductor with corresponding EII of $Z_{eii}(x, y)$ maps onto a point in the w -plane at (u, v_t) on the top plate. The EII is scaled in the w -plane by

$$M(u, v_t)Z_{eii}(x, y) = M(u, v)Z_{eii}(\text{Re}\{f(g^{-1}(u, v_t))\}, \text{Im}\{f(g^{-1}(u, v_t))\}) \quad (3.5)$$

where M is a scaling factor, $g^{-1}(u, v)$ is the inverse of the mapping function, and (u, v_t) is a point on the top plate. The differential series impedance per unit length dZ_{top} of the top plate due to a differential width du is then

$$dZ_{top} = \frac{M(u, v_t)Z_{eii}(u, v_t)}{du} \quad (3.6)$$

where Z_{eii} is the EII at some point (x, y) in the z -plane corresponding to a given point (u, v_t) in the w -plane. With the same procedure the differential series impedance per unit length dZ_{bot} of the bottom plate due to a differential width du is

$$dZ_{bot} = \frac{M(u, v_b)Z_{eii}(u, v_b)}{du} \quad (3.7)$$

where (u, v_b) is a point on the bottom plate. Assuming uniform magnetic fields between two plates and using the transverse resonance technique, the inductance due to a differential width du and a separation $|v_t - v_b|$ is given by

$$dL = \frac{\mu_0 |v_t - v_b|}{du} \quad (3.8)$$

where μ_0 is the permeability of free space. Finally, the total differential series impedance per unit length is

$$dZ_{tot} = dZ_{top} + dZ_{bot} + j\omega dL \quad (3.9)$$

The total series impedance per unit length $Z(\omega)$ for the transmission line can be approximated by the parallel combination of each differential impedance, so

$$Z(\omega) = \left[\int_0^{u_0} \frac{du}{j\omega\mu_0|v_t - v_b| + Z_{eii}(u, v_t)M(u, v_t) + Z_{eii}(u, v_b)M(u, v_b)} \right]^{-1} \quad (3.10)$$

where u_0 is the plate width in the mapped domain. In order to verify this method, the results from low to high frequency have been compared to experiments for different geometries such as mirror symmetric twin conductors and a coplanar waveguide, and good agreement has been obtained between calculated and measured data.

3.2.2 Perturbation Method combined with Conformal Mapping Technique

Previous attempts using conformal mapping to evaluate conductor loss go back to 1958 by Owyang and Wu [28]. At high frequency where the skin depth is far smaller than the conductor thickness current crowds toward the surface and edges of the conductor, and it approaches the current distribution of the lossless perfect conductor. Therefore, the current distribution of the finite thickness conductor is approximately calculated from the known current distribution of the perfect conductor in the mapped domain using the scaling factor, and using the surface impedance and the approximated current distribution of the conductor the ohmic loss of the conductor is obtained through the first-order perturbation method. They applied the technique to examples of coplanar strips and CPW with conductors of finite thickness. Recently this approach was extended to an asymmetric CPW by Ghione [29]. Lewin [30] and Vainshtein [31] use a map of zero-thickness conductors instead of a map of finite thickness conductors to approximately obtain the current distribution for the finite thickness conductor. And to get rid of corner singularities of current density for the

zero-thickness conductor, the integration in loss calculation was carried out upto some distance away from the edges. Referring to Collin [32], the resistance of two conductors can be calculated from the real part of the equation

$$Z(\omega) = \frac{1}{I_{tot}^2} \left[\sum_{k=1}^2 \oint_{l_k} Z_s J_s \cdot J_s^* dl_k \right] + j\omega L_{ext}, \quad (3.11)$$

where Z_s is the surface impedance, l_k is the periphery of each conductor, J_s is the surface current density, and L_{ext} is the external inductance. At high frequency the current density of the perfect conductor is uniform in the mapped parallel plates and the current density is approximated using the scaling factor by

$$J(x, y) = \frac{I_{tot} M}{u_o}, \quad (3.12)$$

where M is a scaling factor at (u, v_t) or (u, v_b) on the mapped parallel plate corresponding to (x, y) in original domain. At high frequency the surface impedance of the flat conductor tends to (2.2). Except in the neighborhood of the conductor edges, (2.2) is appropriate all over the conductor. Since the current distribution approximates that of the perfect conductor, to avoid overestimation error near the edges the position independent surface impedance of (2.2) is used in the vicinity of the edges as well as on the flat surface of the conductor. And the total series impedance is given by

$$Z(\omega) = \frac{1+j}{\sigma \delta u_o^2} \left[\int_0^{u_0} (M(u, v_t) + M(u, v_b)) \right] + j\omega \frac{\mu_o |v_t - v_b|}{u_o}, \quad (3.13)$$

where the second term denotes the external inductance of the transmission line.

Recently, Kuester *et al.* [33, 34] have modified this technique using a generalized transfer impedance boundary condition [17] instead of a standard SIBC to take care of

the interaction between top and bottom sides of the conductors at low frequency, and have numerically calculated the stopping distance with respect to various frequencies and two edge shapes. The results are good at high frequency and reasonable for an example of a CPW at low frequency where the conductor thickness is the order of the skin depth or less, but this modification can not accommodate general structures of various transmission lines in that the stopping distance must be *a priori* determined at every frequency of concern and the current distribution of the perfect conductor is not useful to represent the low frequency current distribution of a conductor having finite conductivity.

On the other hand, Schinzinger and Ametani [35] applied the conformal mapping technique to an eccentric coaxial line and a round wire over a ground plane. This procedure gives an equation of similar form to (3.13). But to avoid point by point evaluation of the scaling factor they use an averaged scaling factor and, therefore, averaged surface impedance in the mapped domain. This can result in significant inaccuracy especially in case of conductors that are closely coupled and in which the proximity effect is dominant.

3.2.3 High Frequency and Low Frequency Limit

In (3.9), EII always tends to (3.14) as the frequency increases, (it is identical to (2.2))

$$Z_{eii}^{hf} = \sqrt{\frac{j\omega\mu}{\sigma}} = \frac{1+j}{\sigma\delta}, \quad (3.14)$$

where δ is the skin depth in the conductor. It defines the surface impedance all over the conductor surface except the edges and becomes position independent. With this

substitution, the high frequency series impedance per unit length for the transmission line is derived from (3.10) to be

$$Z^{hf}(\omega) = \frac{1+j}{\sigma \delta u_o^2} \left[\int_0^{u_0} (M(u, v_t) + M(u, v_b)) \right] + j\omega \frac{\mu_o |v_t - v_b|}{u_o}, \quad (3.15)$$

where the second term corresponds to the external inductance, and the real term of (3.15) is the resistance of the transmission line. Note this expression is exactly the same as (3.13) and, therefore, at high frequency the proposed method is said to include the previous perturbation methods combined with the conformal mapping technique.

As $\omega \rightarrow 0$ (i.e., at low frequency), (3.10) becomes

$$Z^{lf}(\omega) = \left[\int_0^{u_0} \frac{du}{Z_{eii}M(u, v_t) + Z_{eii}M(u, v_b)} \right]^{-1} + j\omega \mu_o |v_t - v_b| \quad (3.16)$$

$$\cdot \left[\int_0^{u_0} \frac{du}{(Z_{eii}M(u, v_t) + Z_{eii}M(u, v_b))^2} \right] \left[\int_0^{u_0} \frac{du}{Z_{eii}M(u, v_t) + Z_{eii}M(u, v_b)} \right]^{-2}$$

If the two conductors are symmetric (i.e., two conductors have identical cross-sections and there exists a line of mirror symmetry between them), then $M(u, v_t) = M(u, v_b)$, $Z_{eii}(u, v_t) = Z_{eii}(u, v_b)$, and the real term of (3.16) can be re-written as

$$Z^{lf}(\omega) = 2 \left[\int_0^{u_0} \frac{du}{Z_{eii}M(u, v_t)} \right]^{-1} + j\omega \mu_o |v_t - v_b| \quad (3.17)$$

$$\cdot \left[\int_0^{u_0} \frac{du}{M^2(u, v_t)} \right] \left[\int_0^{u_0} \frac{du}{M(u, v_t)} \right]^{-2}$$

And, therefore, the total DC resistance per unit length is

$$R_{dc} = 2R_s(0) \left[\int_0^{u_0} \frac{du}{M(u, v_t)} \right]^{-1} \quad (3.18)$$

where $R_s(0) = \text{Re}\{Z_{eii}(\omega = 0)\}$

But for an asymmetric transmission line (3.17) gives low frequency resistance with some error. To compensate for this error, the real term of (3.10) can be normalized by the actual DC resistance of the asymmetric conductors.

At low frequency, the current distribution is dominantly determined by resistance. Therefore, if the perturbational expression of the series impedance is valid at low frequency, then (3.11) becomes

$$Z^{lf}(\omega) = \left[\int_0^{u_0} \frac{du}{Z_{eii}M(u, v_t)} \right]^{-1} + \left[\int_0^{u_0} \frac{du}{Z_{eii}M(u, v_b)} \right]^{-1} + j\omega\mu_0 \frac{|v_t - v_b|}{u_o}. \quad (3.19)$$

The real term of (3.19) gives the low frequency resistance of the transmission line, even though the imaginary term may give poor low frequency inductance. If the transmission line is symmetric and EII substitutes as the surface impedance, then the real term of (3.19) is the same as the real term of (3.17).

3.3 Examples

A simple example is the case of parallel rectangular conductors. One configuration is to put two conductors in parallel as in a parallel plate waveguide, and another configuration is to put them side by side as in coplanar strips. A new type of V-shaped conductor-backed coplanar waveguide (VGCPW) is also analyzed, and a normal coplanar waveguide (CPW) and microstrip lines of normal structure and V-

shaped ground are analyzed and compared with each other. The results are compared to more rigorous solutions of the volume filament method (VFM) [24] and the surface ribbon method (SRM) [21, 22]

3.3.1 Symmetric Twin Rectangular Conductors

For conductors with rectangular cross-section a conformal map is guaranteed to exist, based on a Schwarz-Christoffel transformation. Two rectangular conductors can be mapped into parallel plates by two steps of maps. The first map transforms two conductors from the z -plane into two thin, coplanar strips in the t -plane

$$z(t) = c \int_0^t \sqrt{\frac{(\xi^2 - 1/k_1^2)(\xi^2 - 1/k_2^2)}{(\xi^2 - 1)(\xi^2 - 1/k^2)}} d\xi, \quad (3.20)$$

where c, k_1, k_2 , and k are mapping coefficients and are determined by the separation, width and thickness of the conductors. The second map converts the coplanar strips in the t -plane to the parallel plates in the w -plane

$$w(t) = \int_0^t \frac{d\xi}{\sqrt{(\xi^2 - 1)(\xi^2 - 1/k^2)}}. \quad (3.21)$$

The scale factor from the z -plane to the intermediate t -plane is

$$M(t) = \left| \frac{dt}{dz} \right| = \left| \frac{1}{c} \sqrt{\frac{(t^2 - 1)(t^2 - 1/k^2)}{(t^2 - 1/k_1^2)(t^2 - 1/k_2^2)}} \right| \quad (3.22)$$

and the scale factor from t -plane to w -plane is

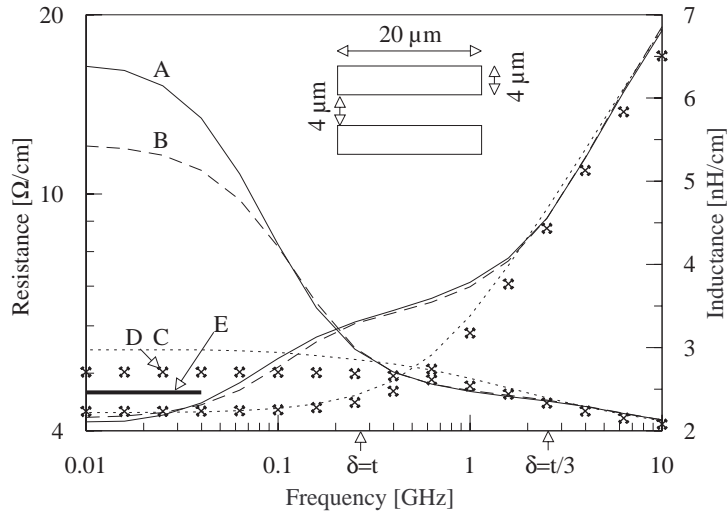
$$N(t) = \left| \frac{dt}{dw} \right| = \left| \sqrt{(t^2 - 1)(t^2 - 1/k^2)} \right|. \quad (3.23)$$

And the series impedance per unit length $Z(\omega)$ is given by

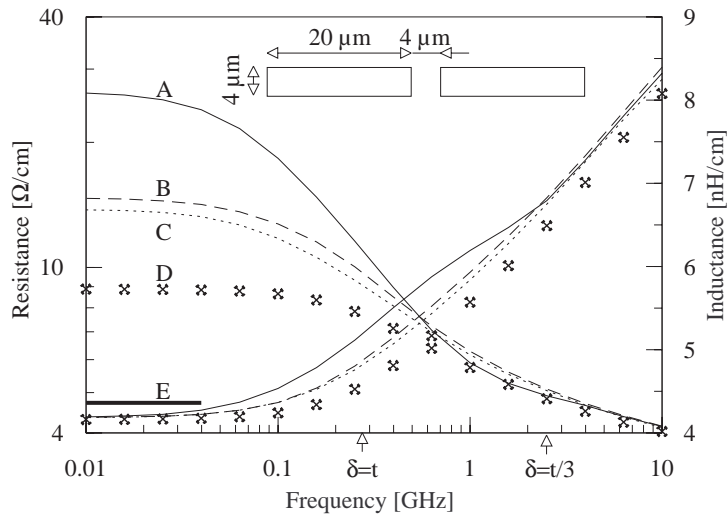
$$Z(\omega) = \left[\int_1^{1/k} \frac{d\xi}{j\omega\mu_o |v_t - v_b| N(\xi) + 2Z_{eii}(\xi)M(\xi)} \right]^{-1} \quad (3.24)$$

To compare between results using different EIIs, both the plane wave model and the transmission line model are used to calculate the series impedance.

Figure 3.2(a) shows results for a closely coupled parallel plate structure with thickness of $4 \mu\text{m}$, width of $20 \mu\text{m}$, gap of $4 \mu\text{m}$, and conductivity of $5.8 \times 10^7 \text{ S/m}$. Calculated resistance and inductance at high frequency (where $\delta < t/3$) and low frequency resistance agree well with results of the volume filament method regardless of the EII model used. At mid frequency, resistance using EII models are overestimated by around 30%, and low frequency inductance (the least important parameter) are also overestimated by 25% and 95%, respectively. Figure 3.2(b) shows results for closely coupled coplanar strips with thickness of $4 \mu\text{m}$, width of $20 \mu\text{m}$, gap of $4 \mu\text{m}$, and conductivity of $5.8 \times 10^7 \text{ S/m}$. Again, calculated resistance and inductance at high frequency and low frequency resistance agree well with results of the volume filament method. At mid frequency resistance using the modified plane wave model gives good agreement within a few percent, the resistance using the transmission line model is overestimated by around 20%, and low frequency inductance is also overestimated by 20% using the modified plane wave model and 40% using the transmission line model. For both examples the surface impedance of the coupled conductors, which is numerically calculated using the volume filament method, has been used and resistance is in good agreement with that of the volume filament method for all frequencies. Since (3.19) assumes uniform flux between the parallel plates in the mapped domain at all frequencies it underestimates low frequency inductance. In (3.10) uniform flux is assumed between the parallel plates with differential width of

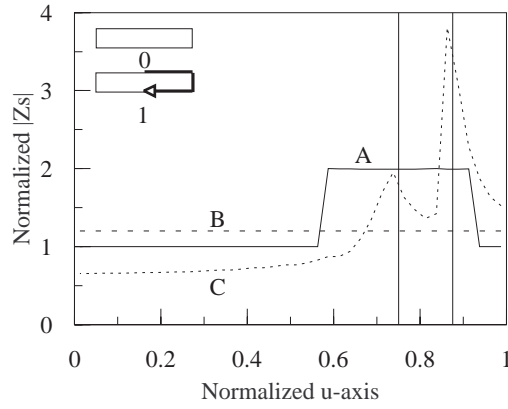


(a) Parallel plate conductors

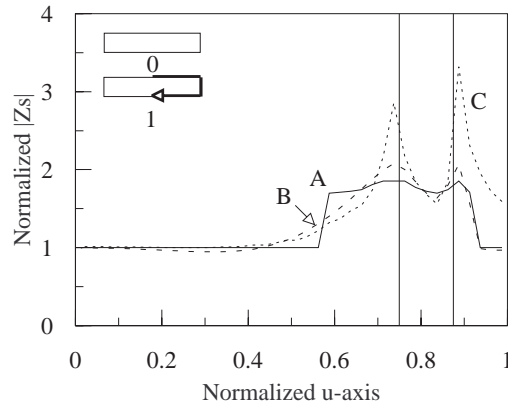


(b) Coplanar strips

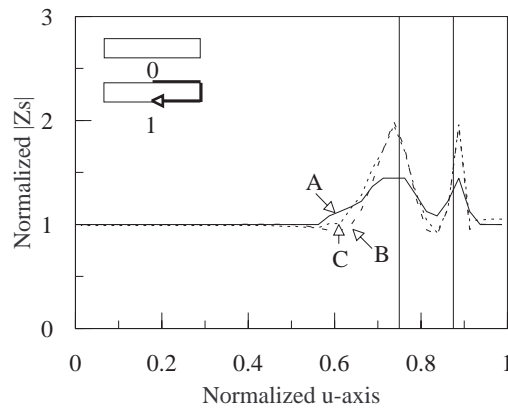
Figure 3.2: Resistance and inductance comparison between the conformal mapping technique with different effective internal impedance models and the surface impedance and the volume filament method for twin rectangular conductors. A(solid line): transmission line model; B(dashed line): modified plane wave model; C(dotted line): the surface impedance; D(*): volume filament method [24]; E(thick solid line): inductance calculation using perturbation method (3.19). 100 integration points used in the mapped domain, 160 unknowns used in VFM.



(a) At the skin depth $\delta=5t$



(b) At the skin depth $\delta=t/2$



(c) At the skin depth $\delta=t/6$

Figure 3.3: Comparison between two effective internal impedance models and the surface impedance for the parallel plate conductors at $\delta = 5t$, $\delta = t/2$, and $\delta = t/6$ ($20 \mu\text{m}$ wide, $4 \mu\text{m}$ thick, and $4 \mu\text{m}$ gap). A(solid line): transmission line model; B(dashed line): modified plane wave model; C(dotted line): the surface impedance.

du in the mapped domain at low frequency, and it also overestimates the low frequency inductance. For both examples the results using the surface impedance give the best answers at all frequencies, but in reality the surface impedance calculation is as intensive as the field calculation and, therefore, EII (an approximation of the surface impedance of an isolated conductor) can be used as an approximation with some tolerable error. For these examples the modified plane wave model gives better results than the transmission line model.

Figure 3.3 compares the surface impedance calculated using the volume filament method with the two EII models, all of which are normalized by the surface impedance of a thin conductor (2.4). At high frequency (i.e., $\delta = t / 6$) the two EII models approach the surface impedance but the modified plane wave model gives better approximation to the surface impedance. At mid frequency ($\delta = t / 2$) the two EII models are close to each other and a little bit deviated from the surface impedance. At low frequency ($\delta = 5t$) the two EII models deviate from the surface impedance, and this deviation accounts for another part of the error in low frequency inductance calculation.

3.3.2 V-shaped Conductor-backed Coplanar Waveguide

Figure 3.4 illustrates a recently proposed coplanar waveguide [42], where the back side ground plane is made V-shaped in order to reduce current crowding and, therefore, to reduce the conductor loss. However, no accurate models for the actual conductor loss in this structure have been reported. Here the attenuation constant is evaluated using a conformal mapping technique.

To determine if the V-groove reduces loss, design constraints must first be set.

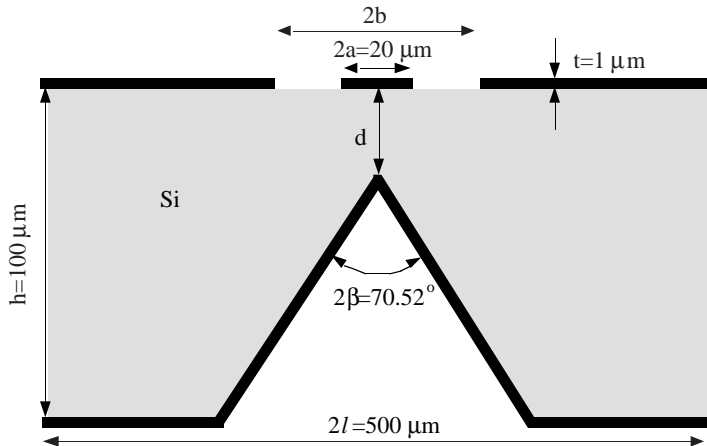


Figure 3.4: V-shaped conductor-backed coplanar waveguide (VGCPW). The angle corresponds to an anisotropically etched groove in (100) Si.

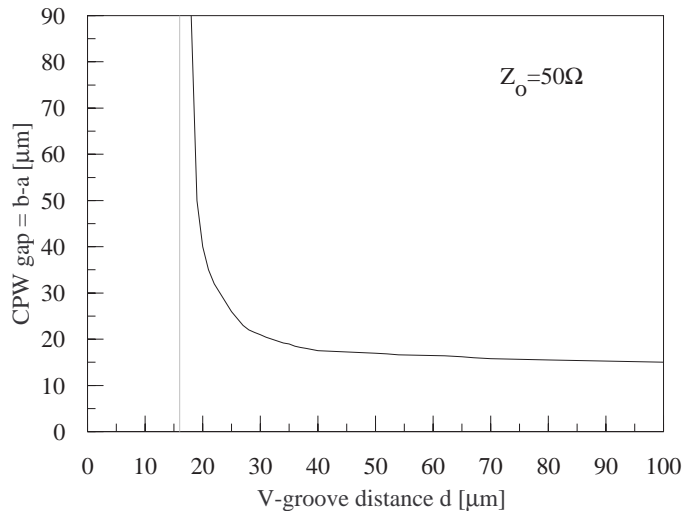
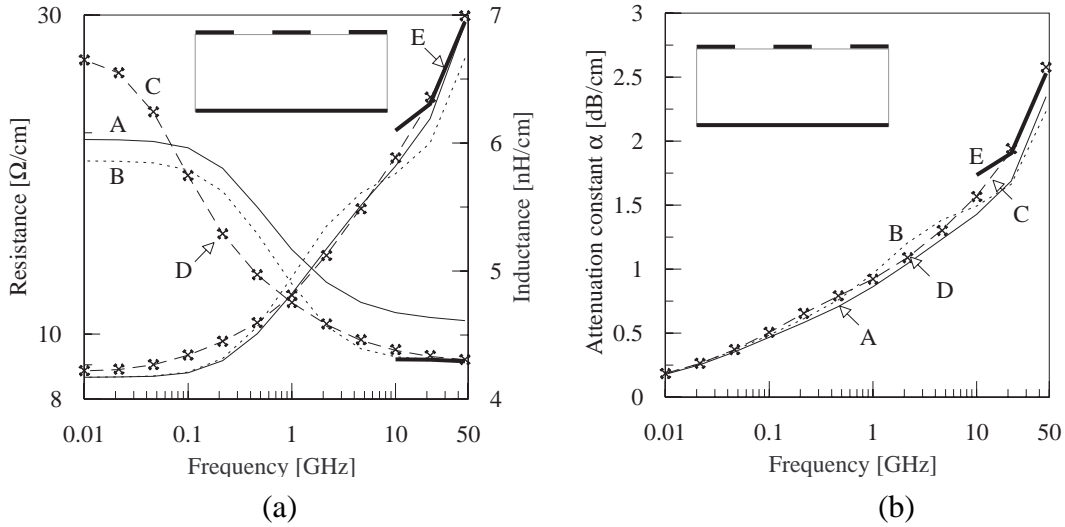


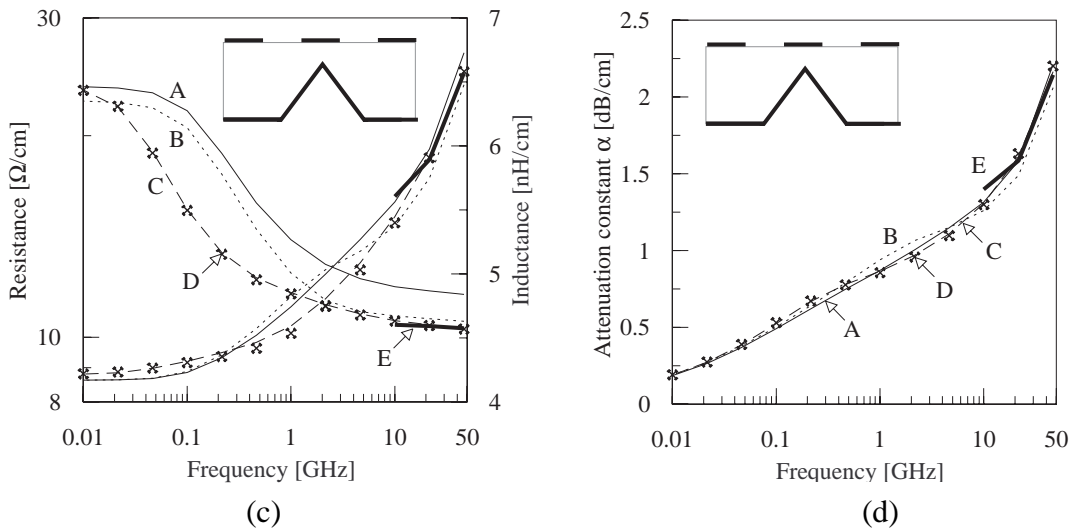
Figure 3.5: CPW gap ($b-a$) as a function of the V-groove distance d for a constant $Z_0 = 50 \Omega$ design. Distance $d = 16 \mu\text{m}$ for a 50Ω V-groove microstrip line (i.e., no CPW ground planes).

Since the center conductor contributes the most to loss, width and thickness of the center conductor is fixed. Width and thickness of the center conductor are $20 \mu\text{m}$ and

$1 \mu\text{m}$, respectively, and the conductivity of metal is $5.8 \times 10^7 \text{ S/m}$, the substrate is high resistivity Si, so dielectric loss is ignored, and the relative permittivity of Si is 11.7. The location of the CPW ground plane (i.e., b) for a specified V-groove (i.e., d and h are given) is determined to maintain a high frequency characteristic impedance of 50Ω . To get designs of 50Ω characteristic impedance, capacitance is calculated using conformal mapping by assuming the air-dielectric boundary is a perfect magnetic wall. The calculated capacitance is compared to the result using the boundary element method (BEM) [43, 44]; the conformal map result considering the thickness of conductors agreed with BEM results to within a few percent ($< 2.5\%$) up to the fairly wide gap ($b - a$) of $90 \mu\text{m}$. Figure 3.5 shows the resulting gap ($b - a$) necessary to maintain 50Ω impedance as a function of the V-groove separation d . Figure 3.6 compares the resistance and loss per unit length calculated with the different methods for a simple conductor-backed CPW ($d = h = 100 \mu\text{m}$, $b - a = 15 \mu\text{m}$) and a 50Ω VGCPW ($d = 20 \mu\text{m}$, $b - a = 40 \mu\text{m}$). As the V-groove gets closer to the center conductor than $20 \mu\text{m}$ the CPW ground plane gap rapidly increases to infinity, i.e., to maintain 50Ω characteristic impedance the structure becomes the pure V-groove microstrip line shown in Fig. 3.7(a). The conformal map including metal thickness slightly over or under estimates resistance within an error of 15% and 5% for a normal CPW and a VGCPW, respectively, but the conformal map assuming zero-thickness metal gives better resistance, within an error of 5% for both cases. Error results from the fact that resistance is normalized to make DC resistance correct and EII is used, not the true surface impedance. For high frequency inductance the conformal map including metal thickness gives good results, but the conformal map assuming zero-thick metal overestimates by 6% for both cases. For comparison, another con-

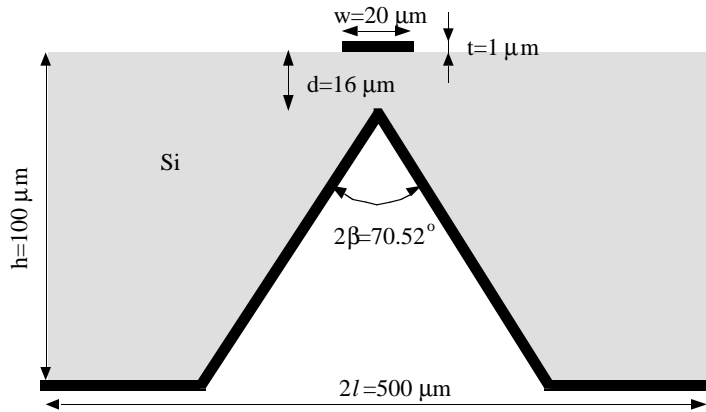


(a) Resistance and inductance and (b) attenuation constant for a 50Ω CPW ($a = 10 \mu\text{m}$, $b = 25 \mu\text{m}$, and $d = h = 100 \mu\text{m}$).

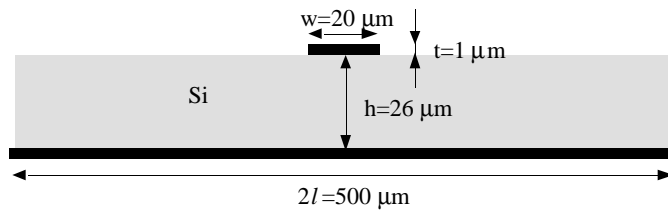


(c) Resistance and inductance and (d) attenuation constant for a 50Ω CPW ($a = 10 \mu\text{m}$, $b = 50 \mu\text{m}$, $d = 20 \mu\text{m}$, and $h = 100 \mu\text{m}$).

Figure 3.6: Comparison of various modeling techniques for the conductor loss of a 50Ω CPW and a 50Ω VGCPW. A(solid line): conformal map assuming conductor thickness is zero; B(dotted line): conformal map of finite thickness conductors; C(dashed line): surface ribbon method [21, 22]; D(*): volume filament method [24]; E(thick solid line): perturbation method (3.13).



(a) A 50 Ω microstrip line with V-shaped ground plane



(b) A 50 Ω microstrip line

Figure 3.7: A 50 Ω microstrip line with V-shaped ground plane, designed using the boundary element method (BEM) [43, 44] and a 50 Ω microstrip line, designed using reference [26].

formal mapping technique based on the perturbation method of (3.14) is used to get high frequency resistance, and good agreement is obtained for both cases.

For a simple microstrip of 50 Ω and the pure V-groove microstrip in Fig. 3.7, conductor losses are also calculated and the design of a simple 50 Ω microstrip line is acquired based on reference [26]. Figure 3.8 shows the resistance per unit length with different methods for a 50 Ω microstrip line. The conformal map including metal thickness and using EII of rectangular conductor overestimates resistance for all fre

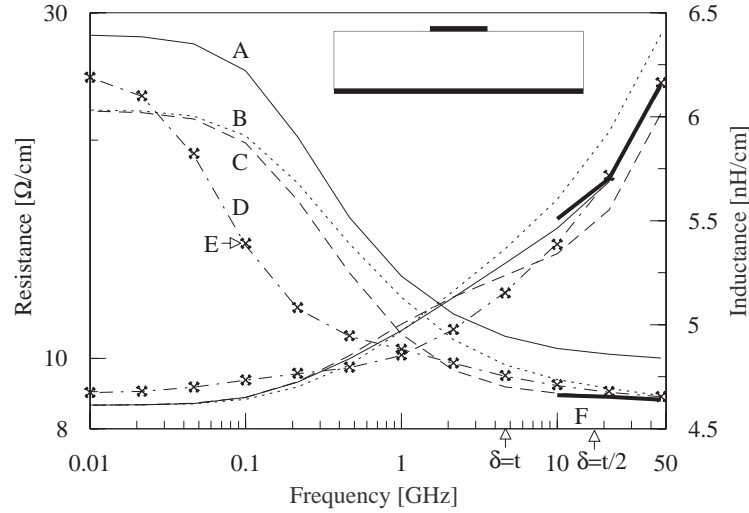
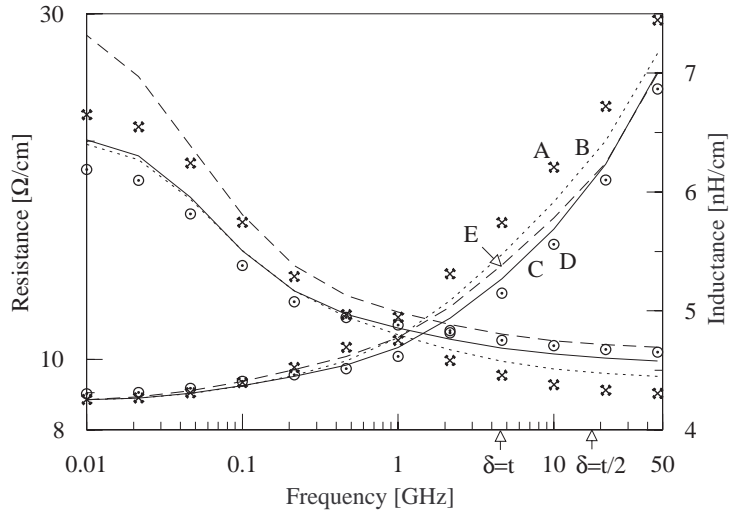
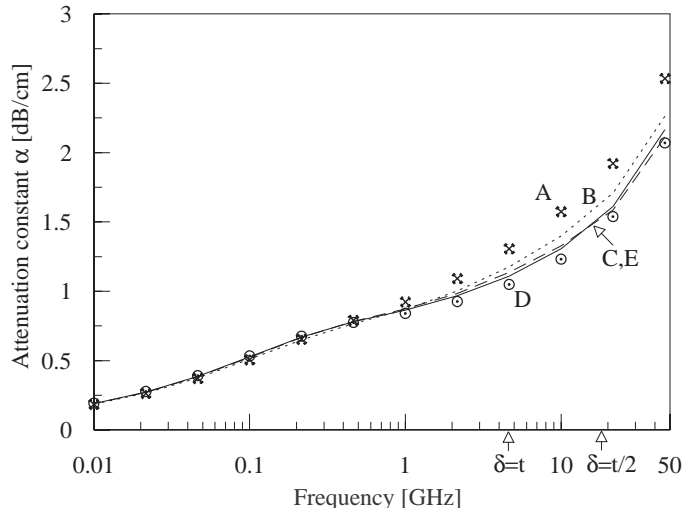


Figure 3.8: Comparison of various modeling techniques for resistance and inductance of a 50Ω microstrip line. A(solid line): conformal map assuming conductor thickness is zero; B(dotted line): conformal map of finite thickness conductors using the effective internal impedance of the rectangular conductor; C(dashed line): conformal map of finite thick conductors using the effective internal impedance of the flat conductor; D(dot-and-dashed line): surface ribbon method [21, 22]; E(*): volume filament method [24]; F(thick solid line): perturbation method (3.14).

quencies within an error of 17%, the conformal map including metal thickness and using EII of flat conductors underestimates high frequency resistance by 9% and overestimates mid frequency resistance with a 10%, and the conformal map assuming zero-thick metal gives good resistance for all frequencies except at mid frequency of 10% overestimation. And high frequency resistance calculated from perturbation method agrees well with rigorous quasi-static solutions. For high frequency the conformal map assuming zero-thick metal overestimates inductance by 4%. Figure 3.9 shows a comparison of the resistance and loss for different 50Ω designs, ranging from pure CPW, to pure V-groove microstrip, to a simple microstrip. The high fre



(a) Resistance and inductance for various 50Ω designs



(b) Attenuation constant for various 50Ω designs

Figure 3.9: Comparison of conductor loss for several 50Ω designs. A(\times): $b - a = 15 \mu\text{m}$ $d = 100 \mu\text{m}$ (normal 50Ω CPW); B(dotted line): $b - a = 21 \mu\text{m}$ $d = 31 \mu\text{m}$ (50Ω VGCPW); C(solid line): $b - a = 40 \mu\text{m}$ $d = 20 \mu\text{m}$ (50Ω VGCPW); D(\circ): 50Ω microstrip line; E(dashed line): 50Ω microstrip line with V-shaped ground plane.

quency resistance does decrease as the V-groove gap d decreases and CPW gap ($b - a$) increases, eventually approaching that of the simple microstrip line (which here is the minimum loss configuration). For example, at 46.4 GHz the calculated attenuation constant is 2.5 dB/cm for the normal CPW, falling to 2.26 dB/cm for VGCPW with $b - a = 21 \mu\text{m}$ and $d = 31 \mu\text{m}$, or 2.16 dB/cm for $b - a = 40 \mu\text{m}$ and $d = 20 \mu\text{m}$; for comparison, the calculated loss for simple 50Ω microstrip was 2.07 dB/cm (20 μm wide and 1 μm thick strip, 26 μm high over ground plane). For constant characteristic impedance designs, the VGCPW does show some reduction in loss at high frequencies, although the rather small reduction may not justify the added complexity of fabrication.

For the volume filament method and the surface ribbon method the impedance matrix is first filled once (pre-process) and solved at each frequency, and for conformal mapping the integration points are first searched (pre-process) and the series impedance is calculated easily at each frequency. Table. 3.1 compares run times and corresponding number of unknowns on an IBM RISC 6000 for various conductor loss calculations. This shows that conformal mapping-based models are reasonably accurate as well as numerically efficient for design purposes.

3.4 Discussion and Further Consideration

The conformal mapping technique combined with EII has been shown to be very efficient in evaluating conductor loss for quasi-TEM transmission line mode. This method consists of two parts; first, EII is assigned on the surface of conductor, which represents the internal behavior of the conductor. Second, the conformal map is found for given geometries. In this section SIBC and EII were distinguished, and the

conformal mapping technique based on perturbation and the conformal mapping technique based on transverse resonance were compared. Numerical computation of Schwarz-Christoffel transformation and the limitation of the conformal mapping technique were discussed.

Transmission Line Structure	Method	Number of unknowns	CPU time [sec]	
			Pre-process	Solve per frequency
VGCPW, microstrip	"thin metal" CM	2	8.6*	0.15**
	"thick metal" CM	6	8.6*	0.15**
VGCPW	VFM	1009	300	350
	SRM	265	3	7
microstrip	VFM	599	35	75
	SRM	165	1.4	1.8

Table 3.1: Comparison of run times on an IBM RISC 6000 for various conductor loss calculations. SRM [21, 22] and VFM [24] use gaussian elimination as a matrix solver, *: 24-point Gaussian quadrature with 10 segments between two singular points in conformal maps, **: 100 point integration in the mapped domain.

3.4.1 Standard Impedance Boundary Condition and Effective Internal Impedance

The surface impedance of coupled conductors gives better resistance and inductance than the effective impedance models in case of twin rectangular conductors for all frequencies. At high frequency ($\delta < t/3$), EII models approach the surface impedance regardless of geometries given, and for this frequency range Leontovich boundary condition is satisfied for methods based on perturbation and on transverse resonance. At mid and low frequency, EII is deviated from the surface impedance, the results using EII are a little bit off from the results of other rigorous methods, with

the results using the surface impedance closer to the results of other rigorous methods. This shows that the conformal mapping method with the EII can be used as an approximation to the standard impedance boundary condition (SIBC). In previous work on the perturbation method based on the conformal mapping technique, the generalized transfer impedance has been used to evaluate mid and low frequency instead of the surface impedance of the flat conductors.

Unlike the proposed method where the varying current distribution is properly accounted for by the transverse resonance method from uniform at DC to crowding towards the corner and surface of the conductor at high frequency, the previous perturbation method based on conformal mapping technique should know the current distribution of the conductor at low and mid frequency as well as at high frequency to accurately evaluate the conductor loss for all frequencies. This makes it hard to widely use the perturbation method based on conformal mapping technique.

3.4.2 Integration and Parameter Evaluation in Schwarz-Christoffel

Transformation

To numerically calculate the hyperelliptic integrals, the integration interval along each side of the conductors is divided into 10 segments and 24-point Gaussian quadrature is used at each interval. Gaussian procedure is good enough for many integration problems, but to compute the integral having singular points with a tolerable accuracy a large number of points is inevitable. As explained in [45, 46], Gauss-Chebyshev and Gauss-Jacobi quadrature formulas properly consider singular vertices in the integral and, therefore, appear to be a good choice in the hyperelliptic integrals. Also, much more clever partitioning of the integration interval can be derived as in [46], where the long integration interval between singular points is divided into three

parts with a suitable length ratio and separate integrations are performed on those parts with the minimal Gauss-Jacobi quadrature points. These scheme should reduce the integration time quite a bit.

In the hyperelliptic integrals of Schwarz-Christoffel maps, the mapping coefficients should be *a priori* known before computing the series impedance, and various iterative optimization schemes can be used to find the mapping coefficients. In the study, the Powell method [46] is used, which is a direct search method and one of least-square methods with constraints. There are many direct search methods such as the Peckham method, the Hooke and Jeeves method, etc., and all of them can be adopted to coefficient evaluation with some gain or loss. Gradient methods, as well as direct search methods, can be used; for example, the steepest descent method, Newton's method [47], Newton-Raphson Method [45], etc. Both approaches need initial guess of the coefficients and the advantage of the gradient method over the direct search method lies in accurate computation of derivatives.

3.4.3 Limits of Proposed Conformal Mapping Technique

For planar transmission lines such as a microstrip line, a coplanar strip line, a coplanar waveguide, etc. the proposed conformal mapping technique has proven to be quite useful in evaluating the conductor loss. But for multi-conductor (i.e., more than two) transmission lines, a conformal map does not result in a simple parallel plate, and, therefore, the proposed conformal mapping technique is no longer useful. As in reference [48], planar multi-conductor transmission lines can be mapped into cylindrical multi-conductor lines. But even for that simplified geometry calculating self and mutual capacitance is no longer straightforward and easy. And it necessitates a

more generalized technique which is still numerically efficient and accurate and is based on more rigorous numerical method than the conformal mapping technique.